DE GENNES PARAMETER DEPENDENCE ON SUPERCONDUCTING PROPERTIES OF MESOSCOPIC CIRCULAR SECTOR

DEPENDENCIA DEL PARÁMETRO DE GENNES SOBRE LAS PROPIEDADES SUPERCONDUCTORAS DE UN SECTOR CIRCULAR MESOSCÓPICO

JOSÉ JOSÉ BARBA ORTEGA

PhD, Universidad Nacional de Colombia, Bogotá, jjbarbao@unal.edu.co

MIRYAM RINCÓN JOYA

PhD, Universidad Nacional de Colombia, Bogotá, mrinconj@unal.edu.co

Received for review November 11 th, 2011, accepted March 9th, 2012, final version March, 16 th, 2012

ABSTRACT: We implemented an algorithm using the link variable method to solve the time dependent Ginzburg-Landau equation in a superconductor prism with circular geometry. The sample is surrounded by a thin layer of another superconductor at higher critical temperature and submitted to an external magnetic field applied perpendicular to its plane. The boundary condition is taken into account with the de Gennes extrapolation length.($b = \sigma(1-\gamma)^{-1}$) We evaluate the magnetization, vorticity, the first, and the third critical thermodynamical fields as functions of the external magnetic field and parameter. γ We found that for these interfaces, the third critical field $\boldsymbol{H_{c3}}(T)$ and magnetization are largely increased while the first critical field $\boldsymbol{H_{c1}}(T)$ remains practically constant.

KEYWORDS: De Gennes parameter, Vortex configuration, Magnetization

RESUMEN: Implementamos un algoritmo usando el método de variables de enlace para resolver las ecuaciones Ginzburg Landau dependientes del tiempo en un prisma superconductor con geometría circular. La muestra está rodeada por una pequeña capa de otro superconductor a mayor temperatura crítica y sometida a un campo magnético externo aplicado perpendicular a su plano. Las condiciones de contorno son tomadas en cuenta con la longitud de extrapolación de de Gennes ($b = \sigma(1-\gamma)^{-1}$) Evaluamos la magnetización, la vorticidad, el primero y tercer campos críticos termodinámicos como función del campo magnético externo y el parámetro γ . Encontramos que para estas interfaces, el tercer campo crítico termodinámico $\boldsymbol{H_{c3}}(T)$ y la magnetización aumentan grandemente mientras el primer campo crítico $\boldsymbol{H_{c1}}(T)$ permanece prácticamente constante.

PALABRAS CLAVE: Parámetro de De Gennes, Configuración de vortices, Magnetización

1. INTRODUCTION

The properties and applications of superconductors are determined by their critical parameters. By nanostructuring a superconductor, one can modify the properties of an existing superconducting structure [1–6]. A way to modify, enhance, or suppress the properties of superconducting samples can be realized by controlling the sample boundary conditions. Theoretically, one can simulate different types of material by varying the de Gennes extrapolation length in the boundary conditions for the order parameter. It is well known that the phenomenology of superconductivity can be described by the time-dependent Ginzburg Landau (TDGL) equations [7–9]. In the present paper we use the TDGL theory to study the magnetization, vortex configuration, and the transition fields in a circular sector with arbitrary shape (see Fig. 1 of [10]). We use an algorithm considering the boundary conditions for the order parameter. Our procedure makes it possible to generalize the algorithm to any circular geometry and value. According to the choice of boundary conditions, we will show that the superconductivity can be considerably enhanced, and a new classification of type-I and type-II superconductor may occur.

2. THEORETICAL FORMALISM

The properties of the superconducting state are usually described by the complex order parameter Ψ for which the absolute square value $|\Psi|^2$ represents the

superfluid density, and the vector potential $\boldsymbol{A}$, which is related to the local magnetic field, as $\boldsymbol{h} = \nabla \times \boldsymbol{A}$. In dimensionless units, the TDGL equations are given by [11–14]:

$$\frac{\partial \Psi}{\partial t} = \frac{1}{\eta}[(i\nabla + \boldsymbol{A})^2\Psi + (1-T)(|\Psi|^2 - 1)\Psi] \quad (1)$$

$$\frac{\partial \mathbf{A}}{\partial t} = -(1-T)Re\{\overline{\Psi}(i\nabla + A)\Psi\} - \kappa^2(\nabla \times \nabla \times \mathbf{A} \quad (2)$$

Equations (1) and (2) were rescaled as follows: Ψ in units of $\Psi_\infty(\mathrm{T})$ lengths in units of $\xi(T)$, $\boldsymbol{H_a}$ in units of $H_{c2}(T)$ in units of $H_{c2}(T)\xi(T)$, temperatures in units of T_c, we use $\eta = 1$The dynamical equations are complemented with the appropriate boundary conditions for the order parameter:

$$\hat{n} \cdot \left(-i\hbar\nabla - \frac{e^*}{c}\boldsymbol{A}\right)\Psi = (1-\gamma)\, i\hbar/\sigma \quad (3)$$

where $\hat{\boldsymbol{n}}$ is the unity vector perpendicular to the surface and directed outward the domain of the superconductor, and σ is the mesh size. This domain is defined by the internal and external radii, $\boldsymbol{r}$ and $\boldsymbol{R}$, respectively, and spans an angular width, which can vary from 0 (slit) to 2π (disc) (see Fig. 1 of [10]). (We will assume that the current density normal to surface does not vanish at the interfaces. We can show that the discrete implementation of this condition is as follows:

$$\Psi_{1,j} = \gamma U_{\rho,1,j}\Psi_{2,j} \quad (4)$$

$$\Psi_{N_\rho+1,j} = \gamma \overline{U}_{\rho,N_\rho,j}\Psi_{N_\rho,j} \quad (5)$$

$$\Psi_{i,1} = \gamma U_{\theta,i,1}\Psi_{i,2} \quad (6)$$

$$\Psi_{i,N_\theta+1} = \gamma \overline{U}_{\theta,i,N_\theta}\Psi_{i.N_\theta} \quad (7)$$

We unify the boundary conditions upon introducing *γ=(1-σ⁄b)*. For convenience, this notation allows us to obtain a better analysis of the results. For more details see [8].

3. RESULTS

The parameters used in our numerical simulations were *κ=2.2.*

The area of the circular sector is S= 49ξ^2*(T)* for angular width $\theta=\pi/2$. The internal radius is *r=ξ(T).* Such that the external radius is given by $R = \sqrt{196/\pi + r^2}$. We have taken the length of the largest unit cell to be no larger than \$0.1ξ*(T)*×0.1ξ*(T)*. Since the order parameter varied most significantly over a distance ξ*(T),* this choice for the grid space is sufficient to pick the variations of *Ψ*. We started from the Meissner state, where *Ψ =1* and ***A***=0 everywhere are taken as the initial conditions. Then we let the time evolve until the system achieves a stationary state. This is done by keeping the external applied magnetic field H_a which is taken constant until the system achieves a stationary state. Next, we ramp up the applied field by an amount ΔH . The stationary solution for $H_a$is then used as the initial state to determine the solution for $\boldsymbol{H_a}$+Δ***H***, and so on. Usually we started fro zero field and increased H_a until the superconductivity is entirely destroyed. We ramp up the applied magnetic field adiabatically, typically in steps of ΔH=10^{-5}.

In Fig., 1 we determined the values of the magnetization for an external magnetic field H_a*=0.28*H_{C2}*(T)* as a function of γ. At this magnetic field, the superconducting sample is still in the Meissner state and will be more pronounced for bigger values of γ. As one can easily notice, the negative magnetization grows with γ. We found a linear behavior of ***M*** as a function of γ, with m=0.0016±0.00001 as the slope.

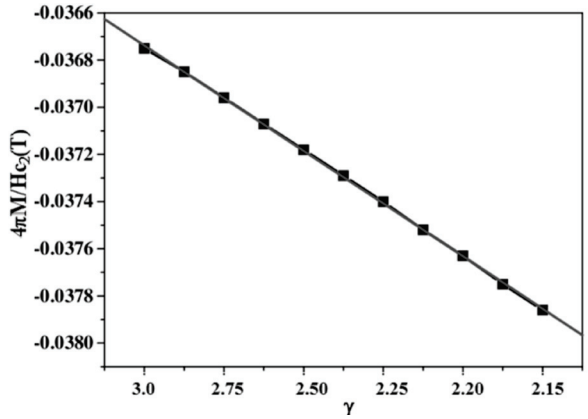

Figure 1. Magnetization as a function of the γ parameter at H_a*=0.28*H_{C2}*(T)*

In Fig. 2, We present the magnetization as a function of the external applied magnetic field H_a for a circular sector for several values of the γ parameter. These curves present a typical profile of a magnetization curve of a mesoscopic superconductor and exhibit a series of discontinuities, in which each jump signals the entrance of one or more vortices into the sample.

Notice that the number of jumps and the transition fields vary significantly with γ.

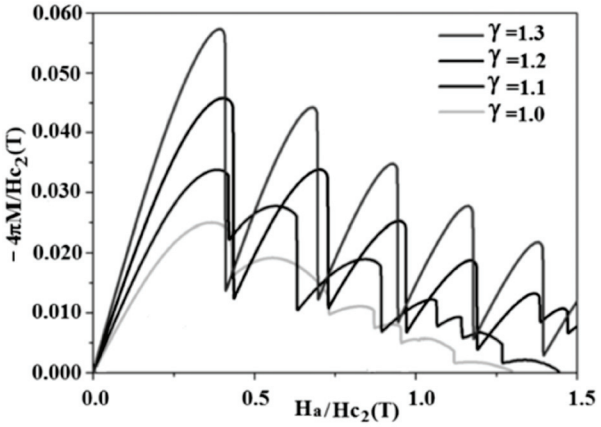

Figure 2. Magnetization curve as a function of the external applied magnetic field for γ=1.0,1.1,1.2,1,3

Another interesting feature is shown for the third critical field $H_{C3}(T)$, the critical field which marks the transition from surface superconductivity to the normal state. In Fig. 3, we present the $H_{C3}(T)$-γ phase diagram for 5 samples with γ=1.0,1.25,2.0,2.5,3.0; we found $H_{C3}(T)$=0.26,0.72,1.63,2.25,2.99 for these cases, respectively. The superconductor/normal transition field $H_{C3}(T)$ grows quickly with γ.

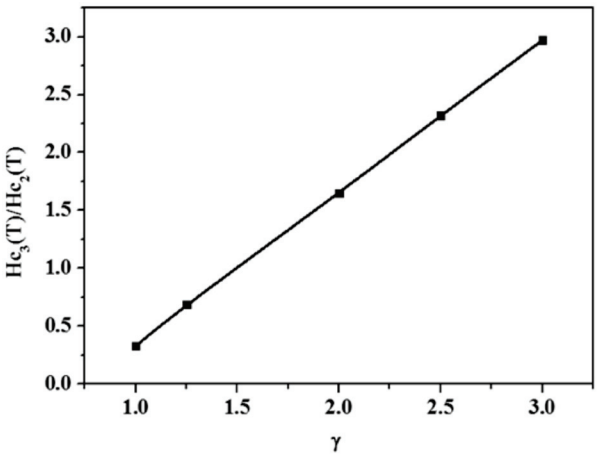

Figure 3. The upper critical field $H_{C3}(T)$ field as a function of the γ parameter

The Cooper pair density as a function of γ is shown in Fig. 4. For these γ values, we observed a power-law behavior, and obtained slope m=-3.33±0.005.

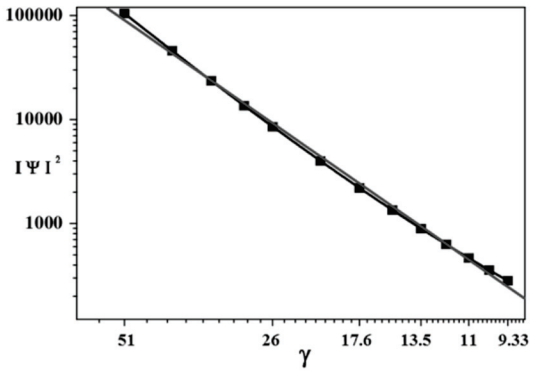

Figure 4. The upper critical field $H_{C3}(T)$ field as a function of the γ parameter

In Figs. 5 and 6, we depict $|\Psi|^2$ for the stationary states with a vorticity equal to 3. We choose different values of the γ parameter to illustrate the role played by the boundary conditions on the properties of the interfaces. We use (a) γ=1.3 at $H_a=0.52H_{C2}(T)$, and (b) γ=1.2 at $H_a=0.42H_{C2}(T)$. In both cases, we have 4 vortices in the sample.

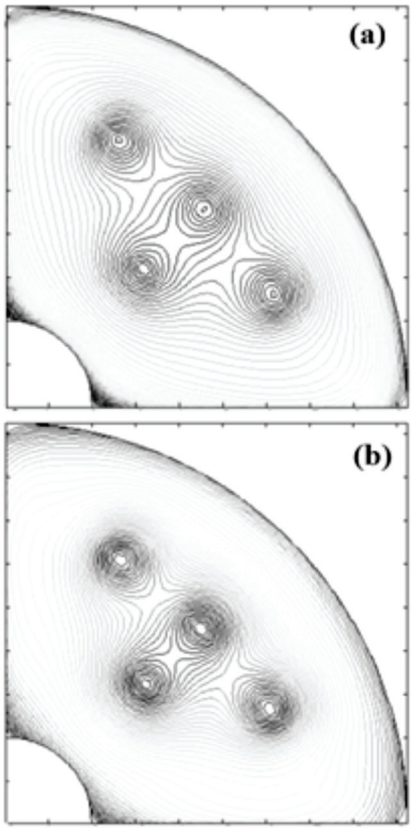

Figure 5. Two-dimensional density contour plot of $|\Psi|^2$ for 3 vortices and the boundary conditions with (a) γ=1.3 at $H_a=0.52H_{C2}(T)$, and (b) γ=1.2 at $H_a=0.42H_{C2}(T)$

In the superconductor/superconductor at higher critical temperature interface we see that $|\Psi|^2$ is strongly enhanced in a region near the surface due to the shielding currents and the Cooper pairs originating from the superconductor of a higher T_c.

4. CONCLUSIONS

In summary, an algorithm has been devised for solving the time-dependent Ginzburg Landau equations for circular geometry and a superconductor/superconductor at a higher critical temperature boundary condition. We have presented some evidence that, if we choose the γ parameter accordingly, we can strongly enhance superconductivity. Also, we found an analytical behavior for the magnetization curve as a function of the γ parameters; we obtained $M \sim \gamma$, $H_{C3} \sim \gamma$ and $\langle|\Psi|^2\rangle \sim \gamma$ for this sample.

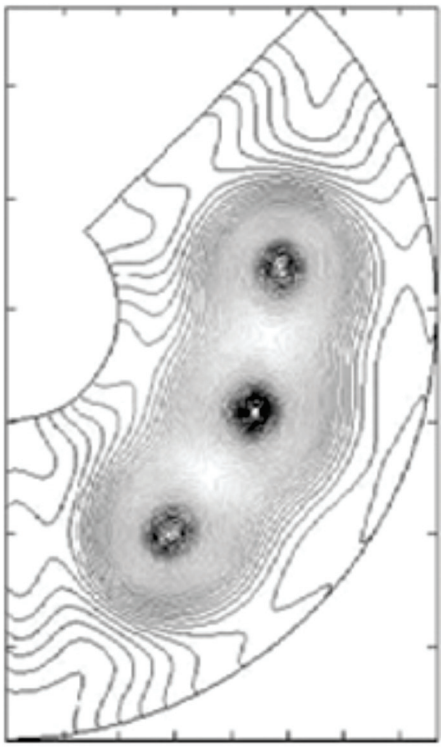

Figure 6. Two-dimensional density contour plot of $|\Psi|^2$ for 3 vortices and boundary conditions with γ=1 at $H_a=0.58H_{C2}$ (T)

ACKNOWLEDGEMENTS

The authors would like to thank Edson Sardella from UNESP-Brasil and LSMA from UFPE-Brasil for their very useful discussions.

REFERENCES

[1] Berdiyorov, G. R., Milosevic, B. J. and Peeters F. M., Stability and transition between vortex configurations in square mesoscopic samples with antidots. Physical Review B, 68, 174521. New York. American Physics Society. 2003.

[2] Puig, T., Rosseel, E., Baert, M., VanBael, M., Moschalkov, V, V. and Bruynseraede, Y., Stable vortex configurations in superconducting 2×2 antidot clusters. Applied Physics Letters, 70, 119118. New York. American Physics Society. 1998.

[3] Puig, T., Rosseel, E., Van Look, E., VanBael, M., Moschalkov, V, V. and Bruynseraede, Y., Vortex configurations in a Pb/Cu microdot with a 2×2 antidot cluster. Physical Review B, 58, 5744. New York. American Physics Society. 1998.

[4] Pogosov, W, V., Vortex phases in mesoscopic cylinders with suppressed surface superconductivity. Physical Review B. 65, 224511. New York. American Physics Society. 2004.

[5] Geim, A, K., Dubonos, S, V., Grigorieva, I, V., Novoselov, K, S., Peeters, F, M. and Schweigert V, A., Non-quantized penetration of magnetic field in the vortex state of superconductors. Nature. 407, pp. 55-57. London, United Kingdom. 2000.

[6] Bruyndoncx, V., Rodrigo, J, G., Puig, T., Van Look, L. and Moshchalkov,V. V., Giant vortex state in perforated aluminum microsquares. Physical Review B, 60, 4285. New York. American Physics Society. 1999.

[7] Barba, J., Sardella, E. and Aguiar, J, A., Superconducting boundary conditions for mesoscopic circular samples. Superconductor. Science and Technology. 24 015001. Washington. 2011. Temperature-dependent vortex matter in a superconducting mesoscopic circular sector. Physica C 470, 1964, Holland. Elsevier, 2010.

[8] Barba, J., Confinement effects on mixed state in superconducting prisms. Dyna, año 78, Nro. 168, pp. 158-163. Medellín, 2011.

[9] Sardella, E., Malvezzi, A, L., Lisboa-Filho P, N. and Ortiz, W., Temperature-dependent vortex motion in a square mesoscopic superconducting cylinder: Ginzburg-Landau calculations. Physical Review B, 74, 014512. New York. American Physics Society. 2006.

[10] Sardella, E. and Brandt, E. H., Vortices in a mesoscopic superconducting disk of variable thickness. Superconductor Science and Technology. 23 025015. Washington. 2010.

[11] Gropp, D., Kaper, H, G., Leaf, G, K., Levine, D, M., Palumbo, M., Vinokur, V. M., Numerical Simulation of Vortex Dynamics in Type-II Superconductors. Journal of Computational Physics 123 (254) Holland. Elsevier. 1996.

[12] De Gennes, P. G., Superconductivity of Metals and Alloys, Benjamin, New York, 1966.

[13] Tinkham, M., Introduction to Superconductivity. McGraw-Hill, New York, 1975.

[14] Buscaglia, G. C., Bolech, C. and López, A., Connectivity and Superconductivity, in: J. Berger, J. Rubinstein (Eds.), Springer, 2000.